Chemical Science

ROYAL SOCIETY OF CHEMISTRY

EDGE ARTICLE

View Article Online
View Journal | View Issue



Cite this: *Chem. Sci.*, 2021, **12**, 2667

All publication charges for this article have been paid for by the Royal Society of Chemistry



# Photoactivatable prodrug for simultaneous release of mertansine and CO along with a BODIPY derivative as a luminescent marker in mitochondria: a proof of concept for NIR image-guided cancer therapy†

Rajeshwari Tiwari,‡[ae] Prashant S. Shinde,‡[b] Sreejesh Sreedharan, ‡[c] Anik Kumar Dey,[ae] Katherine A. Vallis, *[c] Santosh B. Mhaske, *[be] Sumit Kumar Pramanik *[ae] and Amitava Das *[d]

Received 14th November 2020
Accepted 22nd December 2020

DOI: 10.1039/d0sc06270g

rsc.li/chemical-science

Controlled and efficient activation is the crucial aspect of designing an effective prodrug. Herein we demonstrate a proof of concept for a light activatable prodrug with desired organelle specificity. Mertansine, a benzoansamacrolide, is an efficient microtubule-targeting compound that binds at or near the vinblastine-binding site in the mitochondrial region to induce mitotic arrest and cell death through apoptosis. Despite its efficacy even in the nanomolar level, this has failed in stage 2 of human clinical trials owing to the lack of drug specificity and the deleterious systemic toxicity. To get around this problem, a recent trend is to develop an antibody-conjugatable maytansinoid with improved tumor/organelle-specificity and lesser systematic toxicity. Endogenous CO is recognized as a regulator of cellular function and for its obligatory role in cell apoptosis. CO blocks the proliferation of cancer cells and effector T cells, and the primary target is reported to be the mitochondria. We report herein a new mitochondria-specific prodrug conjugate (**Pro-DC**) that undergoes a photocleavage reaction on irradiation with a 400 nm source (1.0 mW $cm^{-2}$) to induce a simultaneous release of the therapeutic components mertansine and CO along with a BODIPY derivative (**BODIPY(PPH$_3$)$_2$**) as a luminescent marker in the mitochondrial matrix. The efficacy of the process is demonstrated using MCF-7 cells and could effectively be visualized by probing the intracellular luminescence of **BODIPY(PPH$_3$)$_2$**. This provides a proof-of-concept for designing a prodrug for image-guided combination therapy for mainstream treatment of cancer.

## Introduction

One of the major emphases of the current therapy and clinical medicine is improving the drug efficacy through the development of an appropriate prodrug that helps in optimizing the absorption, distribution, metabolism, excretion, and unwanted toxicity of the parent drugs.[1–3] A prodrug refers to a pharmacologically inactive compound that yields the active drug in the presence of an exogenous or endogenous stimulus in the form of a chemical or metabolic process.[4–7] An anticancer prodrug should ideally be transported to the specific organelle of the neoplastic cells and undergo stimuli-responsive activation to yield a cytotoxic drug.[8,9] Light-activatable and organelle-specific anticancer prodrugs are comprised of an anticancer drug that is linked to an organelle-directing reagent through a light-responsive, self-immolative linker for controlled drug release in the presence of light as the stimulus.[10,11] Such prodrugs are expected to improve the therapeutic index by a specific release of the payload at the cancer cells—more specifically at the desired organelle to improve the local concentration of the chemotherapeutic around the cells/tumors for minimizing the damage to surrounding healthy tissues.[4,12] Designing such a prodrug has primarily relied on antibody–drug conjugates with the obvious preference for binding of the prodrug to cell-surface receptors that overexpress at the targeted tumors.[13–15] Available knowledge-base about the intricate

[a]*Central Salt and Marine Chemicals Research Institute, Bhavnagar, Gujarat, India. E-mail: sumitpramanik@csmcri.res.in*

[b]*CSIR-National Chemical Laboratory, Pune 411008, India. E-mail: sb.mhaske@ncl.res.in*

[c]*Oxford Institute for Radiation Oncology, University of Oxford, Oxford OX3 7DQ, UK. E-mail: katherine.vallis@oncology.ox.ac.uk*

[d]*Indian Institute of Science Education and Research Kolkata, Mohanpur 741246, West Bengal, India. E-mail: amitava@iiserkol.ac.in*

[e]*Academy of Scientific and Innovative Research (AcSIR), Ghaziabad 201002, India*

† Electronic supplementary information (ESI) available: The synthesis and characterization data of **Pro-DC**. See DOI: 10.1039/d0sc06270g

‡ These authors contributed equally.

synthetic methodologies as well as the organelle specificity of certain reagents could help researchers in designing an appropriate prodrug for organelle-specific release of the drug in its active form. For image-guided therapy, it is also important to design a prodrug that simultaneously liberates a luminescent marker in its luminescence ON state along with the active drug.[16,17] Such a prodrug design would enable one to achieve improved drug efficacy along with the option for visualization of intracellular processes and target-specific drug delivery.[18,19]

Mertansine, a benzoansamacrolide, is known to be a highly potent microtubulin inhibitor and binds at or near the vinblastine-binding site to induce mitotic arrest in cells and prevents the formation of mature microtubules.[20] The efficacy of this drug was thoroughly examined in preclinical and clinical settings.[21] Data generated through several phase I and phase II clinical trials with patients having diverse types of cancers revealed a substantially high systematic toxicity in humans to gainsay any desired therapeutic benefits at tolerable doses. However, the potent cytotoxicity of mertansine can be utilized in a targeted delivery approach for the selective destruction of neoplastic cells, and all efforts in developing an efficient prodrug using mertansine are limited to the designing of an antibody–drug conjugate.[22] Microtubules are an integral part of mitochondria and the release of mertansine at mitochondria offers an attractive choice for treating hyperproliferative diseases.[23,24] Carbon monoxide (CO) is increasingly being recognized as an immunoprotective and homeostatic molecule and mitochondria have been proposed to be a major site of action for carbon monoxide.[25,26] Thus, designing a mitochondria-specific prodrug that leads to the simultaneous release of mertansine and CO, apart from achieving improved pharmacokinetic parameters, offers an effective therapeutic strategy.[27–31] Arguably, mitochondria-targeted drug delivery also helps in combating drug resistance.[30,32] Following a similar notion, we are reporting herein a prodrug (**Pro-DC**), a drug-small molecule conjugate having mertansine covalently linked to a luminophore (**BODIPY($PPh_3$)$_2$**) through a light-cleavable spacer for achieving the stimulus-responsive release of the drug mertansine in its active form.

Literature reports suggest that the appropriate choice of the phenacyl functionality as the sulfhydryl protecting group allows wavelength-controlled photolysis of the thioester linkage (–S–(CO)–O–B, B is a benzyl derivative) to yield the corresponding sulfhydryl derivative with subsequent loss of the gas transmitter CO moiety.[33–35] This methodology was adopted for designing the desired prodrug for the present study. Such an example of a light-induced organelle-specific release of a potent drug from a physiologically more benign prodrug is scarce in the contemporary literature.

The prodrug **Pro-DC** is composed of two moieties that are linked covalently by a light-cleavable thioester linkage (Scheme 1). The first component is a BODIPY based fluorescent probe that shows a strong luminescence in the NIR region ($\lambda_{Ems}$ = 660 nm; $\lambda_{Ems}$ = 0.51) and is linked with a tubulin disrupting cancer growth blocker maytansinoid through a thioester linkage. Additionally, the presence of the lipophilic

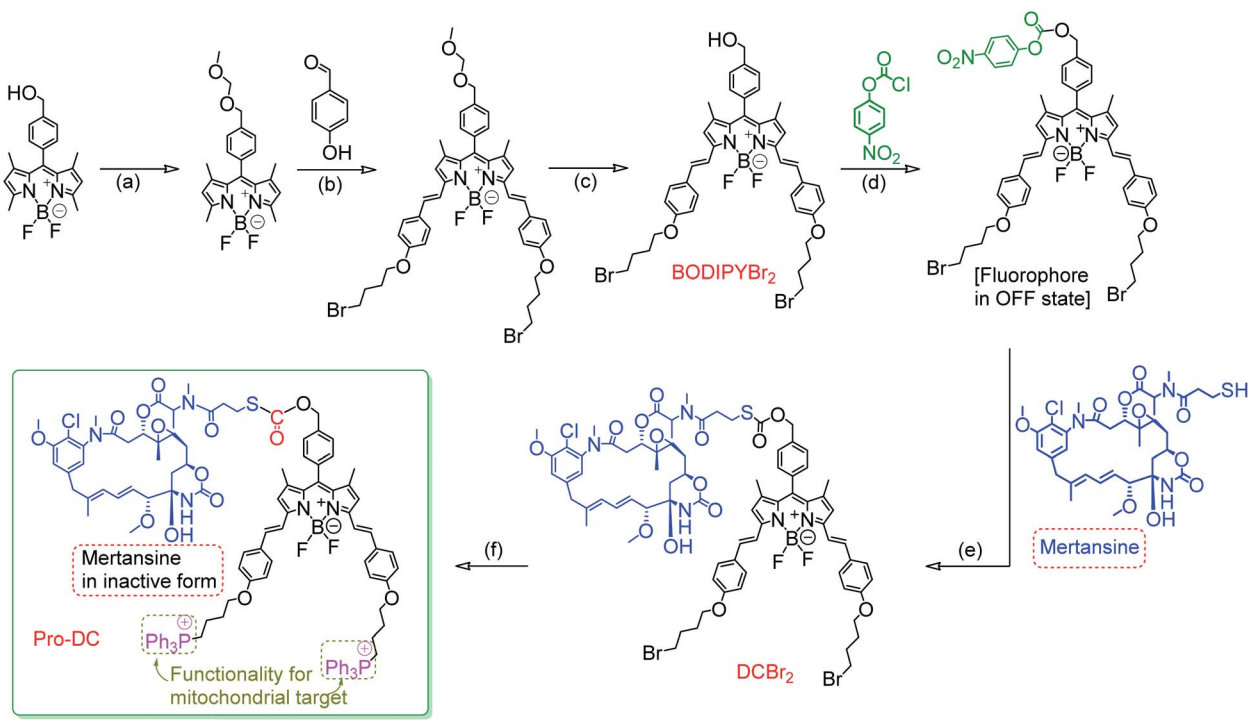


Scheme 1 The molecular structures of mertansine, **$BODIPYBr_2$**, **$DCBr_2$**, **Pro-DC** and **BODIPY($PPh_3$)$_2$** and intermediates that were used for the synthesis of the theranostic prodrug **Pro-DC**. Cleavage of the S–C bond in the thioester functionality on irradiation with 400 nm light is also indicated. (a) Chloromethyl methyl ether, DIPEA; (b) (i) 4-hydroxy benzaldehyde, piperidine, AcOH and (ii) 1,4-dibromobutane, $K_2CO_3$; (c) 4 N HCl in 1,4-dioxane (d) 4-nitrophenyl chloroformate, DIPA; (e) mertansine; (f) $PPh_3$.

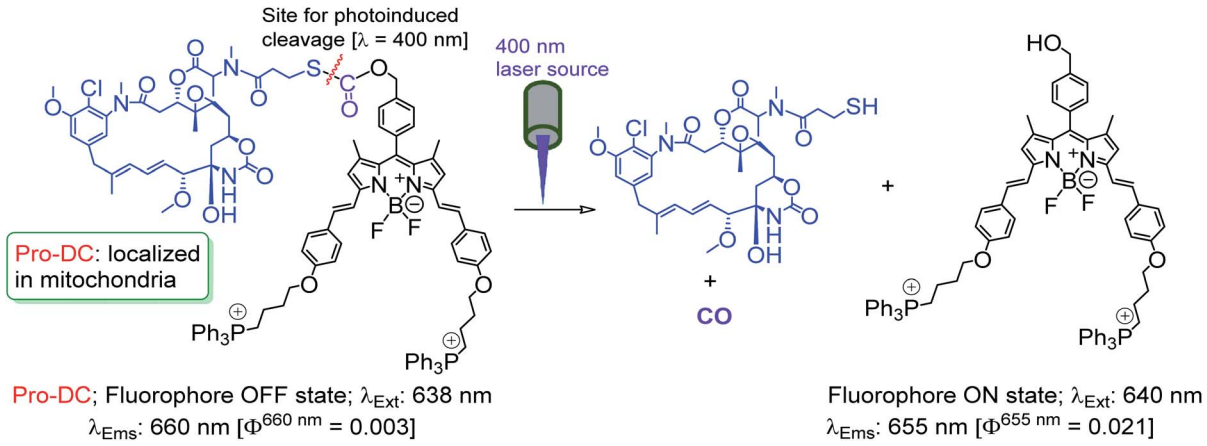


Scheme 2 Proposed photo-induced activation mechanism of **Pro-DC**.

triphenylphosphonium salt functionality in **Pro-DC** could account for its preferential localization in mitochondria. On irradiation of the **Pro-DC** with visible light, the sulfaneyl linkage was ruptured and resulted in the release of the luminescent moiety **BODIPY(PPh$_3$)$_2$** for bio-imaging and free maytansinoid in its active form for chemotherapy. Localization of **Pro-DC** in mitochondria and the light-induced release of mertansine and CO in this organelle of MCF-7 cells are attributed to its enhanced chemotherapy efficiency compared to free mertansine (Scheme 2).

## Results and discussion

The detailed synthetic methodology for **Pro-DC**, **BODIPYBr$_2$**, **BODIPY(PPh$_3$)$_2$** and other intermediates, along with their various analytical and spectroscopic characterization data are discussed in the Experimental section (ESI†). Spectroscopic and analytical data ensured the desired purity of the prodrug (**Pro-DC**) and all isolated intermediates, including **BODIPY(PPh$_3$)$_2$**. BODIPY conjugate, **Pro-DC** was found to be soluble in water, and accordingly, the absorption spectrum of **Pro-DC** was recorded in an aqueous HEPES buffer solution (pH = 7.4).

An intense absorption band with a maximum at 640 nm ($\varepsilon$ = 30 000 L mol$^{-1}$ cm$^{-1}$) was observed, and this was attributed to an $S_0$–$S_1$ electronic transition associated with the BODIPY moiety (Fig. S1†). **Pro-DC** showed a weak luminescence band with a maximum at ~660 nm ($\lambda^{660\ nm}$ = 0.003, BODIPY was used as the standard) upon excitation at 640 nm. Presumably, an extended conjugation at the α-position of each of the two pyrrole rings favored a facile intra-molecular charge-transfer (ICT) process and the observed bathochromic shift for the respective absorption and emission band. A facile ICT process would account for a narrow HOMO–LUMO energy gap and its poor emission quantum yield.[36–38] Apart from mertansine, **BODIPY(PPh$_3$)$_2$**, the other crucial product of the photolysis process, was also synthesized. Electronic spectral data recorded for **BODIPY(PPh$_3$)$_2$** revealed an absorption maximum at 638 nm ($S_0$–$S_1$ transition) and a luminescence maximum at 655 nm ($\lambda^{655\ nm}$ = 0.21 for $\lambda_{Ext}$ of 638 nm). Presumably, the absence of the inhibitory influence of mertansine as the luminescence quencher in **BODIPY(PPh$_3$)$_2$** accounts for its switch ON luminescence response, as compared to **Pro-DC**. Thus, luminescence spectral data tend to support the *in situ* generation of mertansine and **BODIPY(PPh$_3$)$_2$** under physiological conditions on irradiation with a 400 nm light source. To verify this proposition, prodrug **Pro-DC** was irradiated with a 400 nm LED source (continuous source, blue LED; 1.0 mW cm$^{-2}$). The luminescence spectral profile for 1 μM of **Pro-DC** solution under physiological conditions (10 mM aq. HEPES buffer, pH 7.4) was recorded as a function of time (Fig. 1). A steady increase in luminescence intensity at ~660 nm was observed. The luminescence spectral profile was recorded for about 60 min until no appreciable spectral change was observed. A plot of $F_t/F_0$ ($F_0$ is the initial intensity and $F_t$ is the intensity at a specified time of irradiation) at 660 nm as a function of time is shown in Fig. 1b. A control experiment was performed in the dark while maintaining all other experimental conditions unchanged. The results of this control experiment are shown in Fig. 1b, which confirms that there is no change in emission intensity at 660 nm. Importantly, the luminescence spectral profile of the photolyzed solution matched closely with that of **BODIPY(PPh$_3$)$_2$**. This further corroborated our presumption that irradiation with 400 nm LED light induced a photocleavage at the thioester linkage (–S–/–(CO)–O–B) to yield mertansine (the potent drug) and **BODIPY(PPh$_3$)$_2$**—a luminophore with an appreciable luminescence quantum yield. This also tends to rationalize the switch ON luminescence response when prodrug conjugate **Pro-DC** was subjected to the 400 nm irradiation. Additionally, the release of the luminophore **BODIPY(PPh$_3$)$_2$** was not evident when **Pro-DC** was subjected to dark incubation in the presence of various reducing biothiols (cystine, homocystine, glutathione and NaSH, ESI Fig. S2†). These control experiments confirmed that the prodrug conjugate **Pro-DC** was stable under physiological conditions, as well as towards various biothiols that are common in human physiology. These results confirmed that the release of the luminophore **BODIPY(PPh$_3$)$_2$** could only be achieved through photoactivation of the sulfaneyl linkage.

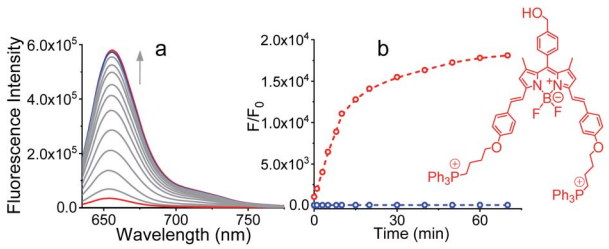


Fig. 1 (a) Emission spectra of **Pro-DC** (1 μM) in aq. HEPES buffer solution (10 mM, pH 7.4) upon irradiation with a blue LED lamp ($\lambda_{irr}$ = 400 nm, 1.0 mW cm$^{-2}$) at 25 °C. Irradiation times: 0, 1, 4, 6, 10, 20, 30, 40, 50, 60 and 70 minutes, respectively. The emission ($\lambda_{Em}$ = 660 nm with $\lambda_{Ext}$ = 640 nm). (b) Relative change in emission intensity ($F/F_0$) at $\lambda_{Em}$ 600 nm as a function of time for **Pro-DC** on irradiation with a 400 nm LED and in the dark: the red coloured trace represents changes on irradiation with 400 nm light and the blue colored trace represents the situation when **Pro-Dc** was kept in the dark.

To ensure that light-induced cleavage at the sulfaneyl linkage resulted in a subsequent release of the potent drug mertansine along with the luminophore **BODIPY(PPh$_3$)$_2$**, detailed HPLC analysis was performed using solutions of pure mertansine, pure **Pro-DC**, **BODIPY(PPh$_3$)$_2$**, the photo-irradiated solution and the control experiment (performed in the dark under identical conditions). Different components that were separated using semi-preparative HPLC experiments were subjected to ESI-MS analysis. Details about the experimental conditions for the HPLC and ESI-MS (positive ion mode) analysis are provided in the ESI.† The HPLC profile of pure mertansine, **Pro-DC** and **BODIPY(PPh$_3$)$_2$** revealed a retention time of 1.98 min ($t_{mertansine}$), 3.47 min ($t_{\mathbf{Pro\text{-}DC}}$) and 7.37 min ($t_{\mathbf{BODIPY(PPh3)2}}$) min, respectively. Then, **Pro-DC** solution was subjected to HPLC after irradiation with a 400 nm LED for 30 min and two new peaks with a retention time of 1.98 min and 7.37 min were observed with a concomitant decrease in the signal for **Pro-DC** having a $t_{\mathbf{Pro\text{-}DC}}$ of 3.47 min. The signal with the retention time of 1.98 min matched with that of pure mertansine recorded earlier and was found to increase when the reaction mixture was spiked with pure mertansine, while that for 7.37 min matched with that of **BODIPY(PPh$_3$)$_2$** (Fig. S3†). The three components (having a retention time of 1.98, 3.47 and 7.37 min) isolated from the photolyzed solution of **Pro-DC** using semipreparative HPLC were subjected to ESI-MS spectral analysis. The mass spectral profile (ESI-MS, positive ion mode) for the component ($t_{Ret}$ = 1.98 min) of the photolyzed solution showed a signal at $m/z$ of 739.10 with the anticipated isotope distribution for mertansine (Fig. S4†). This helped us in confirming the presence of free mertansine in the photo-irradiated solution under physiological conditions. The component having a retention time of 3.47 showed a single peak at $m/z$ 1945.69 (M + H$^+$) with the anticipated isotope distribution for **Pro-DC**. Thus, the component having a retention time of 3.47 in the HPLC profile was unambiguously assigned to unreacted **Pro-DC**. The chromatogram and mass spectral analyses remained unchanged (single peak with a retention time ($t^{dark}_{\mathbf{Pro\text{-}DC}}$) of 3.47 min) when the reaction mixture of the control experiment performed in the dark was subjected to HPLC and mass spectral studies, respectively. This confirmed that **Pro-DC** remained unchanged in experiments that were performed in the absence of 400 nm light irradiation. These results established our proposition that the *in situ* formation of the potent drug mertansine and **BODIPY(PPh$_3$)$_2$** took place on irradiation of **Pro-DC** with a 400 nm LED light source. This also confirmed the proposed mechanistic pathway for the photo-induced reaction. The signal for mertansine having a retention time of 1.98 min was relatively weak and was attributed to the interference from the strong absorbance of **Pro-DC**.

As discussed earlier, CO is being recognized as an endogenous signaling molecule that has potent physiological and therapeutic significance. Literature reports also reveal that mitochondria have been proposed to be a major site of action for CO.[39,40] Thus, targeting mitochondria would allow for CO release at the site of action. Given its high diffusivity, CO should be able to subsequently traverse out of the mitochondria into the cytosol to modulate additional functional effects. The photoresponsive CO release from **Pro-Dc** was confirmed by performing the phosphomolybdic acid–PdCl$_2$ test (Fig. 2 and the ESI†).[41] Under blue light irradiation, CO gas evolves from **Pro-DC** and gets converted into CO$_2$ in the presence of the catalyst PdCl$_2$ with simultaneous reduction of the yellow phosphomolybdic acid to a blue-green colored mixed-valence heteropolymolybdate complex (Mo$^{VI}$–Mo$^{V}$).

After ensuring the efficiency of the photo-triggered degradation of the sulfaneyl linkage and *in situ* release of mertansine along with an NIR-active fluorescent marker, we examined the internalization of **Pro-DC** (1 μM) in live MCF-7 cells (adenocarcinoma, human breast cancer cells) using confocal laser scanning microscopic (CLSM) studies following excitation with a 650 nm laser source. To examine the efficacy of the photo-induced intracellular release of the potent drug, MCF-7 cells were preincubated with **Pro-DC** for 60 min followed by irradiation with a 400 nm LED source (Fig. 3).

The enhanced intracellular luminescence as a function of time on irradiation with 400 nm LED confirmed the release of **BODIPY(PPh$_3$)$_2$** along with the potent drug (mertansine) from **Pro-DC** (Fig. 3). In contrast, MCF-7 cells of the control experiments, incubated with **Pro-DC** (1 μM) in the dark for 60 min, only exhibited a weak basal level of intracellular luminescence. These results confirm the photo-triggered intracellular degradation of the sulfaneyl linkage of the theranostic prodrug, **Pro-**

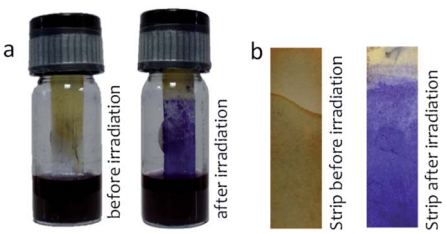


Fig. 2 Experiment for CO elimination. The yellow colour of the strip changed to dark-blue color, indicating the evolution of CO gas from the solution.

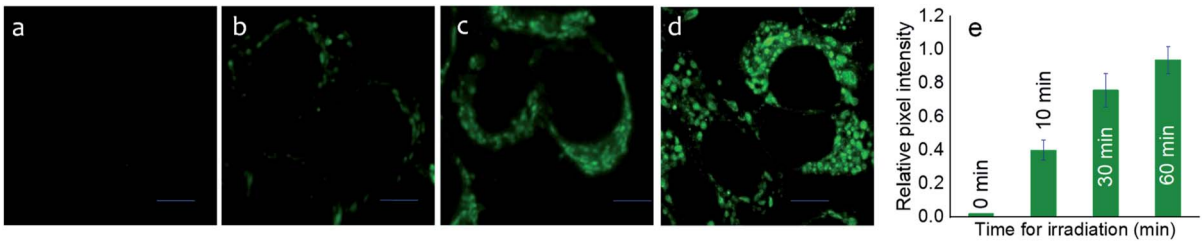


Fig. 3 Cellular fluorescence images of prodrug **Pro-DC**-treated MCF-7 cells. The cells were incubated with **Pro-DC** (1 μM) for 2 h and then irradiated with a blue LED for (a) 0 min, (b) 10 min, (c) 30 min and (d) 60 min. (e) Relative pixel intensity ($n = 3$) from the images. The pixel intensity from the images. The pixel of (d) is defined as 1.0. Scale bar 10 μm. $\lambda_{Ext}$ = 650 nm; $\lambda_{Mon}$ window of 530–710 nm.

**DC** with subsequent release of mertansine and the NIR-active luminophore **BODIPY(PPh$_3$)$_2$** to enable visualization and real-time monitoring of the intracellular chemical process.

Importantly, widefield microscopic images of MCF-7 cells revealed that the prodrug (**Pro-DC**) and the drug (mertansine) are specifically localized in the mitochondria of the MCF-7 cells and this further rationalized our design aspect of having phosphonium ions as an integral part of the prodrug **Pro-DC**. This was further ensured with colocalization studies using a commercially available mitochondria-specific reagent MitoTracker Deep Red. Co-treated cells showed a punctuated intracellular emission from **BODIPY(PPh$_3$)$_2$**, which correlated strongly with the emission from MitoTracker Deep Red (Pearson's coefficient of 0.94; Fig. 4d). Similar colocalization experiments with a commercial lysosome targeting probe (LysoTracker Deep Red) and nuclear counterstain (DAPI) confirmed specific mitochondria localization of the prodrug (**Pro-DC**) and the subsequent *in situ* release of the drug mertansine in the mitochondria of the MCF-7 cells (Fig. S5, S6 and S9†).

Thus, the unique design of the prodrug enabled us to demonstrate a proof-of-concept for developing an efficient prodrug that allows real-time monitoring of the release of the potent drug at the mitochondria of the live MCF-7 cells.

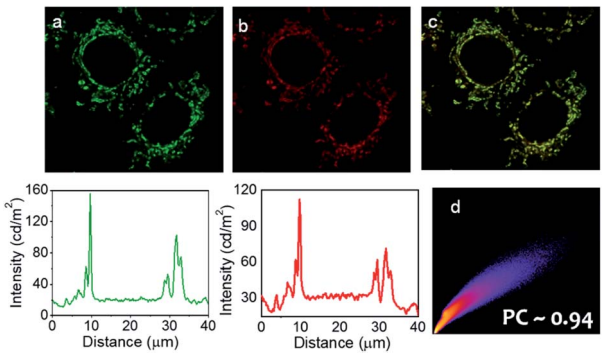


Fig. 4 Colocalization studies of intracellular localization of **Pro-DC** using MitoTracker probes: widefield microscopy images of intracellular emission of **Pro-DC** (panel a) with intensity along the traced line shown underneath. Emission from MitoTracker Deep Red (panel b) and intensity along the same line shown below. The co-localisation of the intensity is shown in panel (c). Panel (c) shows the overlap of the green and red fluorescence, indicating mitochondria localization of **Pro-DC**. Panel (d) shows the Pearson co-efficient = 0.94. Scale bar 10 μm.

The cytotoxicity of **Pro-DC** was quantified by MTT assay using live MCF-7 cells. Concentration-dependent cytotoxicity was observed under blue light irradiation (3.2 mW cm$^{-2}$, 60 min), whereas cells incubated with **Pro-DC** in the dark revealed minimal cellular toxicity (Fig. 5a) over the entire concentration range. A low IC$_{50}$ value of (0.9 ± 0.1) nM was evaluated for **Pro-DC** under photo-irradiation. In comparison, the evaluated IC$_{50}$ value for pure mertansine was evaluated to be (4.2 ± 0.3) nM (Fig. 5a). This signifies enhanced cellular toxicity of the prodrug **Pro-DC** under photo-irradiation, as compared to pure mertansine, as well as that for **Pro-DC** in the dark. Higher efficacy could be attributed to the mitochondria-specific release of the drug. This was further substantiated from the evaluated ratio for the IC$_{50}$ values for **Pro-DC** and **DCBr$_2$** under photo-irradiation; a 4.5 times higher IC$_{50}$ value (IC$_{50}^{\text{Pro-DC}}$/IC$_{50}^{\text{DCBr2}}$) for **Pro-DC** confirmed the role of phosphonium ion in improving the mitochondrial localization, as well as the drug efficacy (Fig. 5b).

The cytotoxicity of **BODIPY(PPh$_3$)$_2$** under identical experimental conditions was found to be insignificant. The phototoxicity index of **Pro-DC** was evaluated at 276 (Fig. S7†). These results confirmed that the mitochondria targeting phosphonium ion helped in specific localization of the prodrug (**Pro-DC**) in mitochondria and the release of the drug mertansine on photoirradiation with a 400 nm light source, as well as improving its efficacy. A control MTT assay was also performed by irradiating live MCF 7 cells in the absence of the prodrug under otherwise identical experimental conditions commonly used for irradiation studies, and no cellular toxicity was observed (Fig. 5). Collectively, these results confirm that the

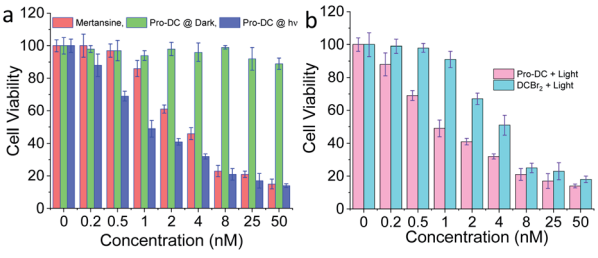


Fig. 5 (a) Viability of MCF-7 cells upon treatment with different concentrations of mertansine and **Pro-DC** under blue light irradiation or in the dark. (b) Viability of MCF-7 cells upon treatment with different concentrations of **Pro-DC** and **DCBr$_2$** under blue light irradiation.

selective mitochondria delivery of mertansine is linked to better drug efficacy.

## Conclusions

In conclusion, conjugation of the anticancer drug mertansine with an NIR-active luminophore (**BODIPY(PPh$_3$)$_2$**) through a light-cleavable sulfaneyl linkage helped us in developing a prodrug (**Pro-DC**) for mitochondria-specific release of the potent therapeutic agents (mertansine) and CO with simultaneous release of the luminophore **BODIPY(PPh$_3$)$_2$** in its luminescence ON state. This luminescence ON response helped in realizing the real-time monitoring of the organelle-specific drug release. The presence of the phosphonium ions in **Pro-DC** helps in achieving the desired permeability through the mitochondrial membrane that has a negative potential. The mitochondrial specificity of **Pro-Dc** helped in localization of mertansine and CO at the mitochondria of the MCF-7 cells. Better individual drug efficacies are reported for mertansine and CO, when these therapeutic reagents are localized in the mitochondria. Recent reports also reveal the positive role of CO in treating neoplastic cells. The prodrug **Pro-DC** shows greatly enhanced cytotoxicity compared to free maytansinoid due to its mitochondria-targeting ability, which can be monitored by cellular and *in vivo* NIR fluorescence imaging. To the best of our knowledge, the observed phototoxicity was the highest (indicated by the lowest IC$_{50}$ value) ever reported for any maytansinoid. These together have contributed to the improved efficacy of the molecular conjugate, **Pro-DC** as compared to free mertansine. Thus, the experimental data helped us in establishing the proof of concept for a photo-responsive NIR-active theranostics application. This present work suggests a molecular design strategy that integrates the key functions of targeting, imaging, release, and treatment within a single agent, which may play an important role in biomedicine.

## Conflicts of interest

There are no conflicts to declare.

## Acknowledgements

Financial support from SERB grants (EMR/2016/001850 and JCB/2017/000004) and a DBT (India) grant (BT/PR22251/NNT/28/1274/2017) is acknowledged by A. D. This manuscript bears CSMCRI registration number 217/2020. Financial support from DST (DST/INSPIRE/03/2017/002477) is acknowledged by R. T.

## Notes and references

1 T. A. Baillie, *Chem. Res. Toxicol.*, 2008, **21**, 129–137.
2 L. W. Peterson and C. E. McKenna, *Expert Opin. Drug Delivery*, 2009, **6**, 405–420.
3 A. F. Stepan, V. Mascitti, K. Beaumont and A. S. Kalgutkar, *RSC Med. Chem.*, 2013, **4**, 631–652.
4 J. Rautio, N. A. Meanwell, L. Di and M. J. Hageman, *Nat. Rev. Drug Discovery*, 2018, **17**, 559–587.
5 X. Li, Y. Hou, J. Zhao, J. Li, S. Wang and J. Fang, *Chem. Sci.*, 2020, **11**, 3215–3222.
6 J. Rautio, H. Kumpulainen, T. Heimbach, R. Oliyai, D. Oh, T. Järvinen and J. Savolainen, *Nat. Rev. Drug Discovery*, 2008, **7**, 255–270.
7 S. Pal, V. Ramu, N. Taye, D. G. Mogare, A. M. Yeware, D. Sarkar, D. S. Reddy, S. Chattopadhyay and A. Das, *Bioconjugate Chem.*, 2016, **27**, 2062–2070.
8 X. Wang, X. Wang, S. Jin, N. Muhammad and Z. Guo, *Chem. Rev.*, 2019, **119**, 1138–1192.
9 W. Liu, H. Liu, X. Peng, G. Zhou, D. Liu, S. Li, J. Zhang and S. Wang, *Bioconjugate Chem.*, 2018, **29**, 3332–3343.
10 Q. Pei, X. Hu, X. Zheng, S. Liu, Y. Li, X. Jing and Z. Xie, *ACS Nano*, 2018, **12**, 1630–1641.
11 A. M. L. Hossion, M. Bio, G. Nkepang, S. G. Awuah and Y. You, *ACS Med. Chem. Lett.*, 2012, **4**, 124–127.
12 A. Dal Corso, L. Pignataro, L. Belvisi and C. Gennari, *Chem.–Eur. J.*, 2019, **25**, 14740–14757.
13 N. Joubert, C. Denevault-Sabourin, F. Bryden and M. C. Viaud-Massuard, *Eur. J. Med. Chem.*, 2017, **142**, 393–415.
14 K. C. Nicolaou and S. Rigol, *Acc. Chem. Res.*, 2019, **52**, 127–139.
15 Y. Matsuda, K. Yamada, T. Okuzumi and B. A. Mendelsohn, *Org. Process Res. Dev.*, 2019, **23**, 2647–2654.
16 H.-W. Liu, X.-X. Hu, K. Li, Y. Liu, Q. Rong, L. Zhu, L. Yuan, F.-L. Qu, X.-B. Zhang and W. Tan, *Chem. Sci.*, 2017, **8**, 7689–7695.
17 X. Xie, B. Li, J. Wang, C. Zhan, Y. Huang, F. Zeng and S. Wu, *ACS Appl. Mater. Interfaces*, 2019, **11**, 41875–41888.
18 J. M. Lambert and C. Q. Morris, *Adv. Ther.*, 2017, **34**, 1015–1035.
19 M. Lopus, *Cancer Lett.*, 2011, **307**, 113–118.
20 M. Lopus, E. Oroudjev, L. Wilson, S. Wilhelm, W. Widdison, R. Chari and M. A. Jordan, *Mol. Cancer Ther.*, 2010, **9**, 2689–2699.
21 W. C. Widdison, S. D. Wilhelm, E. E. Cavanagh, K. R. Whiteman, B. A. Leece, Y. Kovtun, V. S. Goldmacher, H. Xie, R. M. Steeves, R. J. Lutz, R. Zhao, L. Wang, W. A. Blättler and R. V. J. Chari, *J. Med. Chem.*, 2006, **49**, 4392–4408.
22 A. W. Tolcher, L. Ochoa, L. A. Hammond, A. Patnaik, T. Edwards, C. Takimoto, L. Smith, J. de Bono, G. Schwartz, T. Mays, Z. L. Jonak, R. Johnson, M. DeWitte, H. Martino, C. Audette, K. Maes, R. V. J. Chari, J. M. Lambert and E. K. Rowinsky, *J. Clin. Oncol.*, 2003, **21**, 211–222.
23 S. Fulda, L. Galluzzi and G. Kroemer, *Nat. Rev. Drug Discovery*, 2010, **9**, 447–464.
24 W. X. Zong, J. D. Rabinowitz and E. White, *Mol. Cell*, 2016, **61**, 667–676.
25 R. Motterlini and L. E. Otterbein, *Nat. Rev. Drug Discovery*, 2010, **9**, 728–743.
26 R. Motterlini and R. Foresti, *Am. J. Physiol.: Cell Physiol.*, 2017, **312**, C302–C313.

27 D. Wang, H. Huang, M. Zhou, H. Lu, J. Chen, Y.-T. Chang, J. Gao, Z. Chai and Y. Hu, *Chem. Commun.*, 2019, **55**, 4051–4054.
28 Z.-P. Chen, M. Li, L.-J. Zhang, J.-Y. He, L. Wu, Y.-Y. Xiao, J.-A. Duan, T. Cai and W.-D. Li, *J. Drug Targeting*, 2016, **24**, 492–502.
29 Y. Wang, T. Zhang, C. Hou, M. Zu, Y. Lu, X. Ma, D. Jia, P. Xue, Y. Kang and Z. Xu, *ACS Appl. Mater. Interfaces*, 2019, **11**, 29330–29340.
30 H. Wang, Z. Gao, X. Liu, P. Agarwal, S. Zhao, D. W. Conroy, G. Ji, J. Yu, C. P. Jaroniec, Z. Liu, X. Lu, X. Li and X. He, *Nat. Commun.*, 2018, **9**, 562.
31 P. A. Andreux, R. H. Houtkooper and J. Auwerx, *Nat. Rev. Drug Discovery*, 2013, **12**, 465–483.
32 H. Singh, S. Sreedharan, E. Oyarzabal, T. S. Mahapatra, N. Green, Y. L. Shih, M. Das, J. A. Thomas, S. K. Pramanik and A. Das, *Chem. Commun.*, 2020, **56**, 7945–7948.
33 H. Hojo and S. Aimoto, *Bull. Chem. Soc. Jpn.*, 1991, **64**, 111–117.
34 N. Kotzur, B. Briand, M. Beyermann and V. Hagen, *J. Am. Chem. Soc.*, 2009, **131**, 16927–16931.
35 H. Katayama and H. Hojo, *Org. Biomol. Chem.*, 2013, **11**, 4405–4413.
36 H. Agarwalla, H. A. Anila, F. Ali, S. R. Pradhan, B. Ganguly, S. K. Pramanik and A. Das, *Chem. Commun.*, 2018, **54**, 9079–9082.
37 F. Ali, H. A. Anila, N. Taye, R. G. Gonnade, S. Chattopadhyay and A. Das, *Chem. Commun.*, 2015, **51**, 16932–16935.
38 H. A. Anila, F. Ali, S. Kushwaha, N. Taye, S. Chattopadhyay and A. Das, *Anal. Chem.*, 2016, **88**, 12161–12168.
39 L. E. Otterbein, F. H. Bach, J. Alam, M. Soares, H. Tao Lu, M. Wysk, R. J. Davis, R. A. Flavell and A. M. Choi, *Nat. Med.*, 2000, **6**, 422–428.
40 L. E. Otterbein, B. S. Zuckerbraun, M. Haga, F. Liu, R. Song, A. Usheva, C. Stachulak, N. Bodyak, R. N. Smith, E. Csizmadia, S. Tyagi, Y. Akamatsu, R. J. Flavell, T. R. Billiar, E. Tzeng, F. H. Bach, A. M. K. Choi and M. P. Soares, *Nat. Med.*, 2003, **9**, 183–190.
41 A. Verma and S. Kumar, *Org. Lett.*, 2016, **18**, 4388–4391.